JACS
JOURNAL OF THE AMERICAN CHEMICAL SOCIETY

ARTICLE

pubs.acs.org/JACS

Transient Dissociation of the Transducer Protein from Anabaena Sensory Rhodopsin Concomitant with Formation of the M State Produced upon Photoactivation

Masato Kondoh,[†] Keiichi Inoue,[†,§] Jun Sasaki,[‡] John L. Spudich,[‡] and Masahide Terazima*[,†]

[†]Department of Chemistry, Graduate School of Science, Kyoto University, Oiwake, Kitashirakawa, Sakyo-ku, Kyoto 606-8502, Japan

[‡]Center for Membrane Biology, Department of Biochemistry and Molecular Biology, University of Texas Medical School, Houston, Texas 77030, United States

Supporting Information

ABSTRACT: Anabaena sensory rhodopsin (ASR), a microbial rhodopsin in the cyanobacterium sp. PCC7120, has been suggested to regulate cell processes in a light-quality-dependent manner (color-discrimination) through interaction with a water-soluble transducer protein (Tr). However, light-dependent ASR−Tr interaction changes have yet to be demonstrated. We applied the transient grating (TG) method to investigate protein−protein interaction between ASR with Tr. The molecular diffusion component of the TG signal upon photostimulation of ASR_{AT} (ASR with an all-*trans* retinylidene chromophore) revealed that Tr dissociates from ASR upon formation of the M-intermediate and rebinds to ASR during the decay of M; that is, light induces transient dissociation of ASR and Tr during the photocycle. Further correlating the dissociation of the ASR−Tr pair with the M-intermediate, no transient dissociation was observed after the photoexcitation of the blue-shifted ASR_{13C} (ASR with 13-*cis*, 15-*syn* chromophore), which does not produce M. This distinction between ASR_{AT} and ASR_{13C}, the two isomeric forms in a color-sensitive equilibrium in ASR, provides a potential mechanism for color-sensitive signaling by ASR.

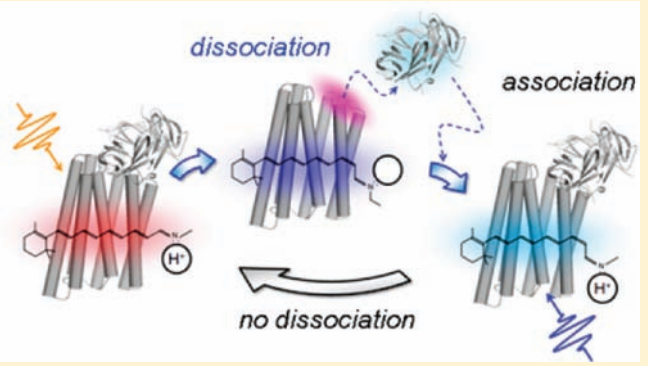

INTRODUCTION

Anabaena sensory rhodopsin (ASR), a retinal-binding membrane protein in the cyanobacterium *Anabaena* sp. PCC7120,[1] is a member of the microbial rhodopsin family,[2] the first-discovered member of which is the light-driven proton pump bacteriorhodopsin (BR). Members of the family have been found in archaea, eubacteria, and unicellular eukaryotes such as fungi and green algae and are recognized by conservation of residues constituting a retinal binding pocket.[3−6] The structures of the rhodopsins crystallized so far, including ASR,[7] are composed of seven transmembrane helices enclosing within the binding pocket a retinylidene chromophore covalently bound via a protonated Schiff base (C═NH) to a lysine residue. The binding pocket accommodates either an all-*trans* or a 13-*cis*, 15-*syn* (C═N *cis*) chromophore, which photoisomerizes at the C_{13} double bond, inducing a series of conformational changes in the protein moiety that are spectroscopically distinguished as intermediate states. The common architecture is responsible for diverse functions, such as light-driven ion transport, light-gated passive ion channel activity, and photosensory reception for phototaxis signals transduced through membrane-bound chemotaxis-receptor-like proteins.[2−6] Thus far, ASR is the only microbial rhodopsin that associates with a water-soluble protein[1,8,9] believed to be a transducer (Tr). On the basis of the photochromic properties of ASR, a pigment with photoactive blue-shifted and red-shifted forms in the dark state, it has been suggested that the ASR−Tr pair regulates color-sensitive processes in the cell, for example, photosynthetic activity, which contains both blue- and red-absorbing pigments.[1]

ASR undergoes chromatic shifts in absorbance to either the red or the blue upon illumination with blue or orange light, respectively. These changes have been attributed to the presence of two species of ASR that accommodate either the all-*trans* (ASR_{AT}) or the 13-*cis*, 15-*syn* (ASR_{13C}) chromophore with the wavelength of the maximum absorption (λ_{max}) red-shifted for the former as compared to the latter (549 nm vs 537 nm, respectively)[1,8] in analogy to the case of BR, which, in the dark-adapted form, exists with two isomeric species in equilibrium. BR with the all-*trans* chromophore undergoes a cyclic reaction upon photoactivation returning to itself, whereas BR with the 13-*cis*, 15-*syn* chromophore is photoconverted to all-*trans* BR, accumulating exclusively the all-*trans* species (light-adaptation of BR). In contrast, the two species of ASR are photointerconvertible,[10] and thus orange light (>570 nm) predominantly converts ASR_{AT} into

Received: March 15, 2011
Published: July 20, 2011

ASR_{13C}, establishing a photostationary equilibrium consisting of 20% ASR_{AT} and 80% ASR_{13C}, whereas blue light (460 nm) shifts the equilibrium to one in which ASR_{AT} predominates. In contrast to BR, dark-adaptation increases the population of ASR_{AT}. The fraction of ASR_{AT} in the dark-adapted condition varies with different experimental conditions (67%,[8] 76%,[7] and 96%[11]).

Time-resolved visible spectroscopy measurements of ASR after photoexcitation have detected a series of conversions between transient intermediate species, analogous to those of all-*trans* BR.[8,12] However, unlike the single cyclic photoreaction of all-*trans* BR, photostimulation of an ASR population induces two separate photochromic reactions, those of ASR_{AT} and ASR_{13C}.[8] Notably, the M state produced by Schiff base deprotonation is formed only in the photoreaction process of ASR_{AT}.[10] The proton transfer reaction appears to be coupled to cytoplasmic-side structural changes involving the C-terminal extension of the ASR protein, judging from the fact that a C-terminal truncation inverts the Schiff-base proton transfer from an unidentified extracellular-side residue in full-length ASR[14] to Asp217 on the cytoplasmic side in the truncated ASR.[12,13] In contrast, in the photoreaction of ASR_{13C}, the Schiff base does not deprotonate (i.e., no M-intermediate forms), and instead a red-shifted species forms before converting into ASR_{AT}.[10]

The association of ASR and Tr has been demonstrated by the effect of Tr in slightly accelerating M-decay,[1] in slightly shifting the absorption spectrum of ASR_{13C} minus ASR_{AT},[8] and also by direct measurement of their dissociation constant by isothermal titration calorimetry (17 μM).[9] For Tr to function as a transducer molecule, it is presumed to alter its binding to ASR upon photoactivation, although no direct evidence has been presented. To explore the dynamics of the protein−protein interaction, here we apply the pulsed laser-induced transient grating (TG) technique, which has been proven to be powerful for detecting dynamics silent to conventional near-UV−visible spectroscopy (spectrally silent dynamics).[15−23] In particular, it has been found that the diffusion coefficient (D) obtained from the TG signals is a very useful property to monitor changing intermolecular interactions with high sensitivity and high time resolution. In the present case of the ASR−Tr system, we observed an increase in D ascribable to release of Tr from the ASR−Tr complex. Because this change was transient during the ASR photocycle, it is not surprising that other techniques without time-resolved capability did not detect this change. The lifetime of the increased D signal coincided with that of the M state during the photoconversion from ASR_{AT} to ASR_{13C}. In contrast, no changes in D were detected during the photoconversion from ASR_{13C} to ASR_{AT}, which produces no M-intermediate. Thus, we suggest that this dissociation is triggered by the conformational change of the cytoplasmic side correlated with the inner protein proton movement during the M-intermediate formation of ASR.

EXPERIMENTAL SECTION

Sample Preparation. Preparations of the full-length ASR and Tr were similar to those described in the previous reports.[1,8] Briefly, the *Escherichia coli* (BL21(DE3), Invitrogen) transformants containing genes for ASR or Tr with a hexahistidine tag introduced at the C-terminus under the *T7* promoter in the plasmid constructs (pET-21d, Novagen) were cultured in 2 × YT medium (37 °C) in the presence of ampicillin (50 mg mL^{-1}). Protein expression was induced by adding 1 mM isopropyl β-D-thiogalactopyranoside (IPTG) and 10 μM all-*trans* retinal. The cell debris was sedimented by low-speed centrifugation (4000*g* or 6000 rpm, BECKMAN COULTER, JA-10), and the membrane fraction in the supernatant was then harvested by ultracentrifugation (150 000*g* or 48 000 rpm, Hitachi Koki, S55A). The membranes were solubilized in buffer solution containing 50 mM Tris-HCl (pH 7.5), 300 mM NaCl, and 1% *n*-dodecyl β-D-maltoside. After centrifugation of the solubilized membranes, the supernatant was incubated with nickel−nitrilotriacetic acid agarose beads (Novagen), and then washed with 50 and 100 mM imidazole in the same buffer, and the protein was eluted with 250 mM imidazole. The eluted protein samples were concentrated and dialyzed to remove the excess imidazole. The Tr was expressed and purified using the his-tag by the same method.

Measurements. The experimental setup for the TG experiment was similar to that reported previously.[20,21] A laser pulse from the second harmonic of a Nd:YAG laser (Spectra-Physics, Model GCR-170-10) (10 ns pulse width) was used as an excitation beam. The spot size of the excitation beams at the sample position was ∼1 mm diameter. The TG signal was detected by a photomultiplier tube (Hamamatsu, R1477) and recorded with a digital oscilloscope (Tektronix, TDS-5052). The grating wavenumber (q) was determined from the decay rate of the thermal grating signal of a calorimetric reference sample, Evans Blue, which gives rise to only the thermal grating signal due to the nonradiative transition within the pulse width of the excitation laser. The q was changed by changing the crossing angle of the excitation pulses and the probe beam. The TG signals were averaged over 9−36 pulses to improve the signal-to-noise ratio. After every shot of the excitation pulse, the sample solution was stirred to avoid significant photoexcitation of the photoproduct. Because the excitation volume (∼1 μL) was much smaller than the sample volume (∼200 μL), the sample condition (contributions of the dark- or light-adapted states) should be constant during the TG measurement. All measurements were carried out at 25 °C.

For the measurement of dark-adapted ASR, a sample solution kept overnight in the dark was used. For light-adaptation, the sample was illuminated with a Xe lamp (USHIO, SX-1500XQ) beam passed through an orange glass filter (>570 nm) and IR cutoff filter for 5 min (the light-adapted ASR sample). The concentration of ASR was 40 μM. To prepare the ASR + Tr solution, the same volumes of ASR (pH 7.5, 80 μM) and Tr (pH 7.5, 560 μM) solutions were mixed. Samples were cleared of particulate matter by centrifugation filtration immediately before measurement.

Principles. The TG signal is generated from the refractive index change (δn) induced by the photoexcitation of the sample by the interference pattern of the two excitation light beams.[22,23] Theoretical descriptions for analyzing the temporal profile of the TG signal are given in section S-1 of the Supporting Information.

RESULTS

TG Signal of ASR without Tr. Before investigating the interaction of ASR and Tr, the TG signal of ASR without Tr was measured. Figure 1 depicts the TG signals observed after photoexcitation of ASR in the absence of Tr under dark-adapted (blue curve) and light-adapted (low intensity red curve) conditions at $q^2 = 4.46 \times 10^{10}$ m^{-2}. Because most ASR under dark-adapted conditions is ASR_{AT} and the TG signal from ASR_{13C} is negligibly weak as described below, this signal represents the TG signal predominantly from the photoreaction of ASR_{AT}. We will first discuss the dark-adapted signal, which consists of an initial rise in the microsecond time range, and decay over a time scale of 100 μs, followed by a large rise−decay feature and a small shoulder signal (∼100 ms time range) before finally decaying to baseline.

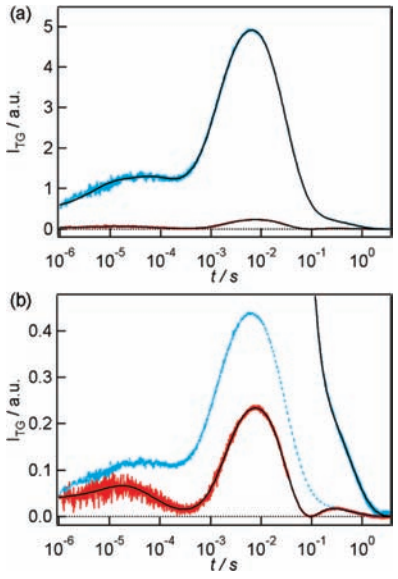

Figure 1. (a) TG signals of dark (blue) and light (red) adapted ASR after photoexcitation at $q^2 = 4.46 \times 10^{10}$ m^{-2} under the same experimental conditions. (b) Magnified signals of (a), and the TG signal of dark-adapted ASR multiplied by $(0.3)^2$ is also shown (blue dotted curve). The black solid curves are the best fitted curves by eq 1 for (a) and by eq 2 for (b), respectively.

The total temporal profile of this signal in the time range of microseconds to seconds was expressed well by the sum of seven exponential functions.

$$I_{TG} = [a_1 \exp(-k_1 t) + a_2 \exp(-k_2 t) + a_3 \exp(-k_3 t) + a_4 \exp(-k_4 t) + a_5 \exp(-k_5 t) + a_6 \exp(-k_6 t) + a_7 \exp(-k_7 t)]^2 \quad (1)$$

where k_i is a decay rate of the TG signal, which indicates the reaction or diffusion kinetics ($k_1 > k_2 > k_3 > k_4 > k_5 > k_6 > k_7$). The pre-exponential factor a_i reflects the refractive index change involved in the reaction with rate k_i. The first and second terms express the initial rise components in the 1 μs to 10 μs time range. The third term reflects the decaying signal in the 100 μs time range. The fourth and fifth terms represent the rise part of the large rise−decay signal in the 1−10 ms time range, and the sixth term represents the decay part. The last term expresses the small shoulder at the last stage of the signal (>100 ms). Fitting parameters to reproduce the signal are listed in Table S1 in the Supporting Information. We repeated the measurements on different days several times and obtained the same values within the experimental error range shown in Table S1.

The assignment of these components was performed using measurements under different grating wavenumbers (q^2). The q^2-independent rate constants are attributable to the reaction kinetics, whereas q^2-dependent rate constants are due to diffusion processes. It was found that k_3 and k_7 depended on q^2 significantly (see Table S2 in the Supporting Information). The value of k_3 agreed well with the value of $D_{th}q^2$ (D_{th}: thermal diffusivity), determined independently from the calorimetric reference sample (Evans Blue) under the same conditions; thus, this component was attributed to the thermal grating signal, that is, $a_3 = \delta n_{th}$, and $k_3 = D_{th}q^2$. Because δn_{th} is negative at this temperature, the signs of the pre-exponential factors were determined as $a_1 > 0$, $a_2 > 0$, $a_4 > 0$, $a_5 > 0$, $a_6 < 0$, and $a_7 < 0$. The significant q^2-dependence of k_7 indicates that this component is the diffusion signal. The q^2-dependence of the other time constants was much less, and the values converged to constant values at small q^2. This behavior could be explained by a combination of reaction rate and diffusion processes (e.g., eq S4 in the Supporting Information). The time constants at small q^2 region (i.e., negligibly small Dq^2 as compared to k_i in eq S4 of the Supporting Information) should represent the kinetics of the reaction. In fact, most of the time constants ($k_1^{-1} = 2$ μs, $k_2^{-1} = 70$ μs, $k_4^{-1} = 1$ ms, $k_5^{-1} = 5$ ms, $k_6^{-1} = 50$ ms) in the small q^2 region ($q^2 = 4.46 \times 10^{10}$ to 1.16×10^{10} m^{-2}) were similar to the previously reported values determined by flash photolysis.[8,12] Therefore, we assigned these kinetic components to the formation and decay processes of the light-induced intermediate species as follows.

$$ASR_{AT} \xrightarrow{2\ \mu s} K \xrightarrow{70\ \mu s} L \underset{5\ ms}{\overset{1\ ms}{\rightleftarrows}} M \xrightarrow{50\ ms} P$$

where P stands for the product species, which was produced after the M-intermediate. Therefore, the characteristic large rise−decay component in the 1−100 ms time range reflects the formation and decay processes of the M-intermediate, which entail a large absorption shift of the spectrum to shorter wavelength due to the deprotonation of the Schiff base. The rate constant k_7 for the last stage of the signal depended on the q^2-value and was not observed in the flash photolysis measurement. This last decay phase therefore reflects the diffusion process of ASR_{AT} (diffusion signal).

It should be noted that the diffusion signal was expressed well by a single exponential function. As reported previously, when the molecular diffusion coefficient (D) of the photoproduct differs from the reactant, the diffusion signals should be expressed by a biexponential function.[15−17] Therefore, the singularity of the diffusion process indicates that D of the photoproduct of ASR_{AT} (ASR_{13C}) remains unchanged. From the equation $k_7 = Dq^2$, we determined D of ASR to be $D = 2.3(\pm 0.3) \times 10^{-11}$ m^2 s^{-1}, which corresponds to a globular protein with a molecular mass around 600 kDa, 20 times larger than that of ASR (e.g., 615 kDa for photochlorophyll−protein complex (2.63×10^{-11} m^2 s^{-1}) and 612 kDa for hemocyanine (2.80×10^{-11} m^2 s^{-1})[24]). The larger than actual value of the molecular weight deduced from the D's is not surprising for membrane proteins, because the protein molecules are embedded in large detergent micelles. Aggregation of the ASR molecules is unlikely because of the independence of the D-value from the sample concentration (not shown).

The TG signal measured after the photoexcitation of the light-adapted ASR is also shown in Figure 1 (red curve). As compared to the TG signal of the dark-adapted ASR, the TG signal drastically changed both in the time profile and, in particular, in the signal intensity (reduced to ~10% in amplitude). As mentioned in the Introduction, although the dominant ASR species in the light-adapted condition is ASR_{13C}, a small fraction of ASR_{AT} (~20%) is present.[1,8] Therefore, the TG signal due to ASR_{AT} as well as ASR_{13C} is superimposed in the TG signal of the light-adapted sample.

The TG signal intensity is proportional to the square of the refractive index change (δn^2) induced by photoreaction. Because the δn is proportional to the concentration, the contribution of the ASR_{AT} to the TG signal in the light-adapted sample as compared to the dark-adapted one is estimated to decrease

to $[\delta n(ASR_{AT})^{light}/\delta n(ASR_{AT})^{dark}]^2 = [20\%/67\%]^2 \approx (0.3)^2$ (using the value 67% for the population of ASR_{AT} in the dark-adapted condition[8]). When the TG signal under the dark-adapted condition is multiplied by $(0.3)^2$ (Figure 1b, blue dotted curve), this signal intensity becomes comparable to that in the light-adapted condition, indicating that the characteristic large rise−decay in the millisecond time range comes from the reaction of ASR_{AT}, which exhibits M-formation and decay. Conversely, ASR_{13C}, which is devoid of M in its photoreaction products as reported previously,[10] contributes little to the TG signal. The small amplitude of the TG signal for ASR_{13C} as compared to that for ASR_{AT} is ascribable to the weaker absorption coefficient[8] and the smaller quantum yield[25] of ASR_{13C}. However, the imperfect match between the TG signal of the light-adapted samples (Figure 1b, red curve) and the estimated TG contribution of ASR_{AT} both in signal intensity and in time profile suggests the presence of refractive index changes during photoreaction of ASR_{13C}. In particular, the TG signal in the light-adapted samples shows a distinct feature in the last decay phase near 100 ms, which is different from TG of ASR_{AT}.

The TG signal was analyzed without separating the ASR_{AT} and ASR_{13C} contributions. The total temporal profile of the signal in the light-adapted condition was reproduced by the sum of seven exponential functions similar to that for the dark-adapted ASR.

$$I_{TG} = [b_1 \exp(-k'_1 t) + b_2 \exp(-k'_2 t) + \delta n_{th} \exp(-D_{th} q^2 t) + b_4 \exp(-k'_4 t) + b_5 \exp(-k'_5 t) + b_6 \exp(-k'_6 t) + b_7 \exp(-k'_7 t)]^2 \quad (2)$$

where $k'_1 > k'_2 > k'_4 > k'_5 > k'_6 > k'_7$ ($k'_2 > D_{th}q^2 > k'_4$ at this q^2). The pre-exponential factor b_i reflects the refractive index change involved in the reaction with rate k'_i. Fitting parameters to reproduce the signal are listed in Table S1 of the Supporting Information. The signal was reproduced well with time constants similar to those obtained in the dark-adapted condition at the same q^2. Some small differences were notable, in particular for k_5 and k_6. These differences may represent a weak contamination of the signal from ASR_{13C} as described above. A significant difference was observed only in the sign of the pre-exponential factor for the last decay phase; the sign was negative in the dark-adapted condition ($a_7 < 0$) and positive in the light-adapted condition ($b_7 > 0$) (see Table S1). Because the decay rate was also q^2-dependent in the light-adapted condition, this last phase should be a diffusion signal. This diffusion signal reflects diffusion processes of both ASR_{13C} and ASR_{AT}, because both of them exist in the light-adapted condition. The same decay rate of the diffusion signal in dark- and light-adapted conditions ($k_7 \approx k'_7$) is consistent with the observation that D of ASR_{13C} is identical to that of ASR_{AT} as described above. On the other hand, the inversion of the sign of the diffusion signal indicates that the refractive index change δn induced by photoreaction of ASR_{AT} is opposite of that from the photoreaction of ASR_{13C}, which is expected because the product for the photoreaction of ASR_{AT} is ASR_{13C}, and vice versa.

Interaction of ASR_{AT} and Tr. The interaction of ASR_{AT} and Tr was studied by measuring the TG signal of ASR in the presence of Tr in dark-adapted samples. For comparison, the TG signals of the dark-adapted ASR in the absence (I_{TG}(ASR)) and presence (I_{TG}(ASR:Tr)) of Tr under the same experimental conditions are depicted in Figure 2a at various q^2-values. It should be noted that most of the temporal profile except for the slowest part of the signal (i.e., the diffusion signal) was not changed by the presence of Tr. For example, the orange line in Figure 2a up to 10 ms (representing the M-formation and decay) is not altered by the presence of Tr. This fact indicates that the reaction process as well as the rate did not depend on the presence of Tr. In a previous measurement, a slight acceleration of M-decay in the presence of Tr was observed when measured in *E. coli* cell suspensions.[1] The difference may be due to the different environment of ASR in vivo.

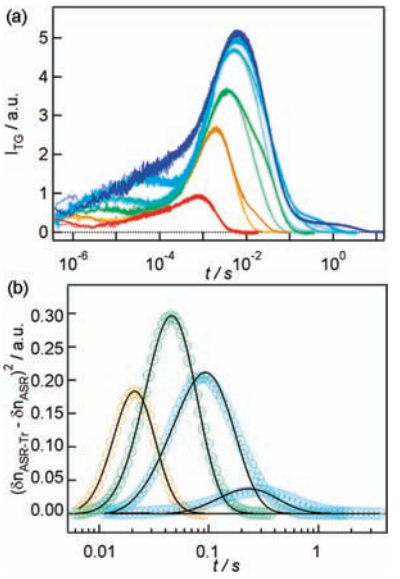

Figure 2. (a) TG signals of the dark-adapted ASR in the absence and presence of Tr at various q^2. The signals at the same q^2 condition are shown by the same colors; $q^2 = 9.84 \times 10^{12}$ m^{-2} (reds), 2.24×10^{12} m^{-2} (oranges), 5.66×10^{11} m^{-2} (greens), 1.84×10^{11} m^{-2} (aquas), 4.46×10^{10} m^{-2} (blues), and 1.16×10^{10} m^{-2} (darker blues). The paler colors depict the TG signal in the absence of Tr, whereas the darker colors represent the signals in the presence of Tr. The signal showed no change in the absorption change parts in the fast time region (up to ~10 ms) between the two samples, while a significant change was observed in the molecular diffusion region at later times. (b) The calculated difference TG signals at various q^2 (TG signals of ASR+Tr sample minus those of the ASR sample under the same q^2 conditions as (a)). The black solid curves are best fits using eq 4. The detailed procedure for the calculation is described in the Supporting Information.

The observed Tr-dependent process is the diffusion signal. For analyzing the Tr-dependent signal, we extracted the difference signal with and without Tr. Because the TG signal intensity is proportional to the square of the refractive index change, taking the difference is not straightforward. We calculated the difference signals by a method described in section S-2 in the Supporting Information and plotted them in Figure 2b.

It is important to note that the difference signals show rise−decay profiles. This profile is a clear indication that there are two diffusing species having different D-values. When the D-value is independent of time, the temporal profile of the species grating signal decays with a molecular diffusion rate for the reactant ($D_R q^2$) and the product ($D_P q^2$). Hence, the time development of the TG signal in the molecular diffusion part can be expressed by a biexponential function:[15−17]

$$I_{TG}(t) = \alpha\{\delta n_P \exp(-D_P q^2 t) - \delta n_R \exp(-D_R q^2 t)\}^2 \quad (3)$$

where $\delta n_R(>0)$ and $\delta n_P(>0)$ are the initial refractive index changes due to the reactant and the product, respectively. Using $\delta n_{th} < 0$, we determined the signs of δn for the rise and decay components as positive and negative, respectively. Hence, the rate constants of the rise and decay components should be $D_P q^2$ and $D_R q^2$, respectively.

Interestingly, the intensity of the difference signal exhibited q^2-dependence; the intensity is weak in a fast time range (<100 ms, large q^2), became stronger in the 100 ms range ($q^2 = 5.66 \times 10^{11}$ m^{-2}), and decreased again in the slower time range (>100 ms). The q^2-dependence of the diffusion signal intensity indicates that there are reaction dynamics in this time range. Therefore, the signal should be analyzed on the basis of the equation representing time-dependent D. However, before analyzing the signal quantitatively, it may be instructive to describe the qualitative features of this signal, because this is quite a unique observation.

The origin of the D-change can be examined from the D-value. We first estimated the D-values with biexponential analysis of the signal using eq 3. From the fitting of the difference signal at $q^2 = 5.66 \times 10^{11}$ m^{-2}, where the signal intensity is largest, D_P and D_R are determined to be $7.5(\pm0.5) \times 10^{-11}$ and $2.5(\pm0.5) \times 10^{-11}$ m^2 s^{-1}, respectively. Because the smaller $D_R = 2.5 \times 10^{-11}$ m^2 s^{-1} is close to that obtained from the signal in the absence of Tr, we attributed this to D of ASR. On the other hand, the larger $D_P = 7.5 \times 10^{-11}$ m^2 s^{-1} was not observed in the absence of Tr. The molecular mass for this diffusion species is expected to be ~50 kDa, for example, comparable to insulin (7.45×10^{-11} m^2 s^{-1}; 47.8 kDa) and pituitary growth hormone (7.36×10^{-11} m^2 s^{-1}; 49.2 kDa).[24] This estimated molecular mass is similar to that of the Tr tetramer (56 kDa), and Tr is known to form a tetramer in solution.[9] Therefore, we attribute the diffusing species of the product to Tr tetramer. Note that, in contrast to ASR, Tr is a water-soluble protein and is not contained in a micelle.

It is important to note that we observed the diffusion of Tr, which does not have a chromophore, upon photoexcitation. We conclude that Tr dissociates from ASR upon photoexcitation of ASR, that is:

$$\mathrm{ASR:Tr} \xrightarrow{h\nu} \mathrm{ASR} + \mathrm{Tr}$$

where ASR:Tr is the complex of ASR and Tr. In this model, three species are involved: ASR:Tr, ASR, and Tr. Because we observed only two diffusion components, the D-values for two of the species should be very similar. This consideration appears to be reasonable. From the D-value of ASR, the effective molecular mass of the ASR micelle is very large, ~600 kDa, as described in the previous section. Upon binding of the Tr tetramer (~50 kDa), the effective molecular mass would change only by ~10%. According to the Stokes–Einstein equation, D of a molecule is inversely proportional to the radius of the molecule. If we assume that the radius is proportional to the cube root of the molecular mass, the change in the molecular mass of ~10% corresponds to the change in the D-value of only ~3%. Hence, the D-values of ASR and ASR:Tr should be very similar to each other. Note that ASR contained in a micelle is expected to be able to interact with the water-soluble Tr, because the hydrophilic cytoplasmic side of ASR provides an aqueous interaction surface for the water-soluble Tr. As stated in the above section, we consider that aggregation of the ASR molecules is unlikely in the micelle. Hence, the ASR:Tr complex might be the 1:1 (transient) complex (where Tr should be a tetramer of the transducer protein).

In this dissociation model, the intensity of the rise–decay diffusion signal reflects the number of ASR:Tr complexes that undergo the light-induced dissociation of Tr. In the milliseconds time range, the signal intensity increases with time. This time-dependence indicates the dissociation reaction proceeds on this time scale. The signal decreases in the time range of tens of milliseconds. This time dependence indicates the back reaction of the dissociation, that is, the association reaction. It is notable that the time scales where the intensity changes by dissociation and association were similar to those of the M-formation (~1 or 5 ms) and M-decay (~50 ms), respectively. This leads to the suggestion that the dissociation and association events are governed by the M-formation and M-decay of ASR.

We quantitatively analyzed the diffusion signal on the basis of the following dissociation and association scheme.

$$\mathrm{ASR:Tr} \xrightarrow{h\nu} \mathrm{ASR^*:Tr} \xrightarrow{k_f} \mathrm{ASR^\dagger} + \mathrm{Tr} \xrightarrow{k_b} \mathrm{ASR:Tr}$$

where subscripts ASR*:Tr stand for the intermediate after photoexcitation but before dissociation of Tr, and ASR† stands for the intermediate after dissociation. The k_f and k_b are the rates for the forward conformation change (dissociation) and for the backward conformation change (association), respectively. On the basis of the above scheme and eq S6 in the Supporting Information with $D_I = D_{R^*} = D_R$, the temporal profile of the TG signal can be given by:

$$\begin{aligned} I_{TG}(t) = \alpha \Bigg[& \left[\delta n_{R^*} - \frac{k_f}{k_f - k_b}\delta n_I - \frac{k_f}{k_f - k_b}\frac{k_f}{(D_R - D_B)q^2 + k_f}\delta n_B + \frac{k_b}{k_f - k_b}\delta n_R \right] \exp\{-(D_R q^2 + k_f)t\} \\ & + \frac{k_f}{k_f - k_b}\left[\delta n_I + \frac{k_b}{(D_R - D_B)q^2 + k_b}\delta n_B - \delta n_R \right] \exp\{-(D_R q^2 + k_b)t\} \\ & + \left[1 - \frac{k_b}{(D_R - D_B)q^2 + k_b} \right] \frac{k_f}{(D_R - D_B)q^2 + k_f}\delta n_B \exp(-D_B q^2 t) \Bigg]^2 \end{aligned} \quad (4)$$

where R, R*, I, and B stand for ASR:Tr, ASR*:Tr, ASR†, and Tr, respectively. We analyzed the difference signals at various q^2 simultaneously using this equation. During the fitting, we used the D(ASR) value obtained in the previous section as D_R. The difference signals were well reproduced by this equation (Figure 2b, black solid curves). Fitting parameters to reproduce the signals are listed in Table S3 in the Supporting Information. We obtained the rates for the dissociation and association to be 8 ($\pm$3) and 80 ($\pm$40) ms, respectively. The measurements were repeated several times over different days, and the same values within the experimental error range. These time constants were similar to those for the M-formation and M-decay. This result strongly suggests that Tr dissociates from ASR only in the M-intermediate during the photoreaction of ASR_{AT}.

Under our experimental conditions shown above ([Tr] = 280 μM, [ASR] = 40 μM), the concentration of the ASR:Tr (Tr as a tetramer) complex is calculated to be 28 μM by using the reported dissociation constant (17 μM). This concentration should be sufficiently large for detection of the Tr dissociation. For additional confirmation of the above model, we increased the Tr concentration further and found that the diffusion signal intensity increased (data not shown), which is consistent with the

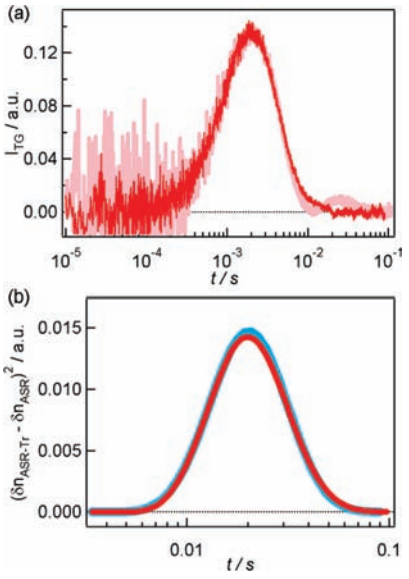

Figure 3. (a) TG signals of the light-adapted ASR in the absence (pink) and presence (red) of Tr at $q^2 = 2.24 \times 10^{12}$ m^{-2}. (b) The difference TG signal (signal of the ASR+Tr minus that of the ASR) in the light-adapted condition under the same q^2 as (a) (red curve), together with the normalized difference signal in the dark-adapted condition (multiplied by 0.9 to show that the kinetics were also similar) under the same experimental conditions (blue curve).

above Tr dissociation model. The time profile did not change by increasing the Tr concentration, probably because the rate constants are determined by the kinetics of the M state with M-formation and decay as the rate-determining steps.

Interaction of ASR_{13C} and Tr. To investigate whether interaction changes occur between ASR_{13C} and Tr during the ASR photoreaction, we compared the effect of Tr on the TG signals of the light-adapted ASR in which ASR_{13C} predominates. Similar to the dark-adapted ASR case described above, Tr-dependent diffusion signals appear in the late-time region (10−100 ms) (Figure 3a). Because light-adapted ASR contains a mixture of ASR_{13C} and ASR_{AT}, the contribution from ASR_{AT} needs to be subtracted. We calculated the ASR_{AT} component on the basis of the amplitude of the 1 ms rise, which is the M-formation-specific TG signal, because M is a photoproduct of ASR_{AT}, but not of ASR_{13C}.[10] The detailed procedures are described in the Supporting Information and Figure S1. The nearly exact match of the diffusion signal normalized for the M-formation-specific TG signal that defines the contribution of ASR_{AT} shows that the diffusion signal is negligible or absent in ASR_{13C} (Figure 3b) (in this figure, the calculated difference signal in the dark-adapted condition was reduced by a factor of 0.9 to show that time profiles were also similar).

Mechanism of Protein−Protein Interaction of ASR with Tr. In this study, we applied the TG technique to investigate the dynamics of protein−protein interaction of ASR with Tr. We observed Tr-dependent transient diffusion coefficient D changes in the sample resulting from the ASR_{AT}, but not ASR_{13C}, isomeric form of the pigment. The appearance of signals with larger D attributable to the release of Tr with an intrinsic time constant of 8 ± 3 ms and the disappearance of the signal at 80 ± 40 ms coincide well with the lifetime of the M-intermediate state of ASR, indicating that Tr is released from the ASR photoreceptor during the lifetime of the M state. The M-intermediate is

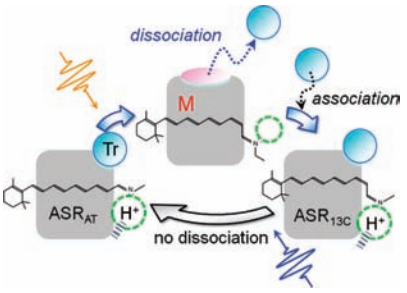

Figure 4. Schematic illustration of the proposed interaction mechanism of ASR with Tr.

produced after photoisomerization of the all-*trans* chromophore in ASR_{AT} to the 13-*cis* form. M-intermediate formation has been shown to entail a deprotonation of the retinylidene Schiff base, a reaction that is coupled to a conformational change in the ASR protein on its hydrophilic cytoplasmic surface and C-terminal extension,[12,14] where Tr is believed to associate. On the basis of the TG results, we suggest that the cytoplasmic-side conformational change triggers the release of Tr from its ASR binding site. With the reprotonation of the Schiff base that follows (M-decay), ASR_{13C} is formed concomitantly with the recovery of the original conformation in the protein moiety, as suggested from the fact that it rebinds Tr. This transient dissociation of Tr does not take place in the photoreaction of ASR_{13C} converting to ASR_{AT}, where M is not produced. A schematic illustration of the possible reactions is shown in Figure 4. The difference in the manner of interactions with Tr during the photoreactions between ASR_{AT} and ASR_{13C} would allow regulation of the concentration of the free Tr in the cells depending on the environmental light condition, for example, light intensity and light wavelength, enabling the ASR to function potentially as a photochromic color sensor.

■ CONCLUSION

The dynamics of the protein−protein interaction between ASR with Tr were investigated by the time-resolved monitoring of the molecular diffusion process. We observed very different features in the TG signals of ASR in the dark- and light-adapted conditions. When Tr was added to the solution, a significant change was observed in the diffusion part of the TG signal, reflecting the change in the molecular diffusion process of ASR induced by the protein−protein interaction. We conclude that this diffusion change reaction reflected the transient dissociation of the Tr from ASR. We found the time constants for the dissociation and subsequent association reactions were similar to those for M-formation (∼5 ms) and M-depletion (∼50 ms) of ASR. Furthermore, this transient dissociation was not observed during the photoreaction of ASR_{13C}, where the M-intermediate is absent. Therefore, we conclude the transient dissociation takes place during M-intermediate formation, when the conformation of the cytoplasmic side is changed after deprotonation of the Schiff base.[12,14] This transient dissociation and association should be a key step for ASR to transmit the photosignal, and differences in the interactions between ASR_{AT} and ASR_{13C} with Tr are likely to be an important mechanism for the function as a photochromic color sensor. Because the ASR absorption spectra do not change upon addition of Tr, it is apparent that the dissociation of Tr is a spectrally silent process and cannot be detected by optical spectroscopy. The TG technique was able to

overcome this limitation and provided this first direct observation of protein−protein interaction dynamics of ASR with Tr.

■ ASSOCIATED CONTENT

Supporting Information. Principles for the TG techniques (section S-1), calculation of the difference signal (section S-2), and fitting parameters (section S-3). This material is available free of charge via the Internet at http://pubs.acs.org.

■ AUTHOR INFORMATION

Corresponding Author

mterazima@kuchem.kyoto-u.ac.jp

Present Addresses

[§]Department of Material Science and Engineering, Nagoya Institute of Technology, Nagoya 466-8555, Japan.

■ ACKNOWLEDGMENT

This work was supported by the Grant-in-Aid for Scientific Research (A) (No. 18205002) and the Grant-in-Aid for Scientific Research on Innovative Areas (Research in a proposed research area) (20107003) from the Ministry of Education, Science, Sports, and Culture in Japan (to M.T.) and by the National Institutes of Health Grant R37GM27750, Department of Energy Grant DE-FG02-07ER15867, and endowed chair AU-0009 from the Robert A. Welch Foundation (to J.L.S.). M.K. was supported by a research fellowship from the Global COE program, International Center for Integrated Research and Advanced Education in Material Science, Kyoto University, Japan.

■ REFERENCES

(1) Jung, K. H.; Trivedi, V. D.; Spudich, J. L. *Mol. Microbiol.* **2003**, *47*, 1513–1522.
(2) Spudich, J. L.; Yang, C. H.; Jung, K. H.; Spudich, E. N. *Annu. Rev. Cell Dev. Biol.* **2000**, *16*, 365–392.
(3) Nagel, G.; Szellas, T.; Kateriya, S.; Adeishvili, N.; Hegemann, P.; Bamberg, E. *Biochem. Soc. Trans.* **2005**, *33*, 863–866.
(4) Spudich, J. L. *Trends Microbiol.* **2006**, *14*, 480–487.
(5) Jung, K. H. *Photochem. Photobiol.* **2007**, *83*, 63–69.
(6) Klare, J. P.; Chizhov, I.; Engelhard, M. *Results. Probl. Cell Differ.* **2008**, *45*, 73–122.
(7) Vogeley, L.; Sineshchekov, O. A.; Trivedi, V. D.; Sasaki, J.; Spudich, J. L.; Luecke, H. *Science* **2004**, *306*, 1390–1393.
(8) Sineshchekov, O. A.; Trivedi, V. D.; Sasaki, J.; Spudich, J. L. *J. Biol. Chem.* **2005**, *280*, 14663–14668.
(9) Vogeley, L.; Trivedi, V. D.; Sineshchekov, O. A.; Spudich, E. N.; Spudich, J. L.; Luecke, H. *J. Mol. Biol.* **2007**, *367*, 741–751.
(10) Kawanabe, A.; Furutani, Y.; Jung, K. H.; Kandori, H. *J. Am. Chem. Soc.* **2007**, *129*, 8644–8649.
(11) Kawanabe, A.; Furutani, Y.; Jung, K. H.; Kandori, H. *Biochem.* **2006**, *45*, 4362–4370.
(12) Shi, L.; Yoon, S. R.; Bezerra, A. G., Jr.; Jung, K. H.; Brown, L. S. *J. Mol. Biol.* **2006**, *358*, 686–700.
(13) Kawanabe, A.; Furutani, Y.; Yoon, S. R.; Jung, K. H.; Kandori, H. *Biochemistry* **2008**, *47*, 10033–10040.
(14) Sineshchekov, O. A.; Spudich, E. N.; Trivedi, V. D.; Spudich, J. L. *Biophys. J.* **2006**, *91*, 4519–4527.
(15) Nakasone, Y.; Eitoku, T.; Matsuoka, D.; Tokutomi, S.; Terazima, M. *J. Mol. Biol.* **2006**, *367*, 432–442.
(16) Tanaka, K.; Nakasone, Y.; Okajima, K.; Ikeuchi, M.; Tokutomi, S.; Terazima, M. *J. Mol. Biol.* **2009**, *386*, 1290–1300.
(17) Hirota, S.; Fujimoto, Y.; Choi, J.; Baden, N.; Katagiri, N.; Akiyama, M.; Hulsker, R.; Ubbink, M.; Okajima, T.; Takabe, T.; Funasaki, N.; Watanabe, Y.; Terazima, M. *J. Am. Chem. Soc.* **2006**, *128*, 7551–7558.
(18) Inoue, K.; Sasaki, J.; Spudich, J. L.; Terazima, M. *Biophys. J.* **2007**, *92*, 2028–2040.
(19) Nakasone, Y.; Eitoku, T.; Matsuoka, D.; Tokutomi, S.; Terazima, M. *Biophys. J.* **2006**, *91*, 645–653.
(20) Terazima, M.; Hirota, N. *J. Chem. Phys.* **1991**, *95*, 6490–6495.
(21) Terazima, M. *Acc. Chem. Res.* **2000**, *33*, 687–694.
(22) Terazima, M.; Hirota, N. *J. Chem. Phys.* **1993**, *98*, 6257–6262.
(23) Terazima, M. *Adv. Photochem.* **1998**, *24*, 255–338.
(24) Sober, H. A. *CRC Handbook of Biochemistry Selected Data for Molecular Biology*; Chemical Rubber Co.: Cleveland, OH, 1968; pp C-10−C-15.
(25) Wada, Y.; Kawanabe, A.; Furutani, Y.; Kandori, H.; Ohtani, H. *Chem. Phys. Lett.* **2008**, *453*, 105–108.